To be published in Optics Letters:

Title: Monostable dissipative Kerr solitons

Authors: Shu-Wei Huang,Eugene Tsao,Yijun Xie,Mingming Nie

Accepted: 30 November 21

Posted 01 December 21

DOI: https://doi.org/10.1364/OL.441165

Monostable dissipative Kerr solitons

EUGENE TSAO[1,*], YIJUN XIE[1], MINGMING NIE[1], AND SHU-WEI HUANG[1,**]

[1] Department of Electrical, Computer, and Energy Engineering, University of Colorado Boulder, 425 UCB, Boulder, CO 80309
[*] eugene.tsao@colorado.edu
[**] shuwei.huang@colorado.edu

Compiled November 25, 2021

Kerr microcombs hold the promise of bringing frequency combs onto the chip and into a variety of applications requiring low size, weight, power, and cost. However, reliable Kerr microcomb generation is hindered by the thermal effect and multistability of dissipative Kerr solitons (DKS). Past approaches toward Kerr microcomb reliability include either deterministic single soliton generation or self-starting soliton behavior but not both. Here we describe a regime of DKS that is *both* deterministic and self-starting, in which only a single soliton can stably exist. We term this new DKS regime "monostable DKS" (MS-DKS) as all other optical behaviors, such as continuous-wave-only and multiple soliton, are fundamentally forbidden by the design. We establish a graphical model to describe MS-DKS and discuss the design principles of MS-DKS. We numerically demonstrate the MS-DKS behavior in an example periodically-poled lithium niobate (PPLN) microring resonator.

http://dx.doi.org/10.1364/ao.XX.XXXXXX

1. INTRODUCTION

The optical frequency comb has revolutionized timekeeping and optical frequency metrology, providing a simple and powerful means of coherently linking radio frequency electronics with optical frequency atomic transitions [1]. Whereas these original frequency combs are formed in tabletop optical cavities, since then, frequency combs have also been found to form in continuous-wave (CW) pumped, high quality factor (Q) nonlinear microresonators [2], a finding that has established the basis for a new kind of frequency comb. These so-called Kerr microcombs rely on a double balance of nonlinearity and dispersion, and (nonlinear) gain and (linear) loss to stably host dissipative Kerr solitons (DKS), the time-domain waveform of this frequency comb. Unique from traditional table-top frequency combs due to high GHz-to-THz repetition rates and low µm-to-mm sizes, Kerr microcombs open new applications for frequency combs, such as highly multiplexed coherent optical communication [3, 4], astrocombs [5, 6], ranging [7], dual-comb spectroscopy [8], integrated frequency synthesizers [9, 10], and optical flywheels [11], all with the hope of chip integration [12].

Despite compelling advantages and promising applications, a significant barrier to the widespread use of Kerr microcombs is unreliable access of the single DKS, which is the preferred time-domain waveform for a smooth frequency comb spectrum. Broadly, efforts to render single DKS generation reliable lie in two categories: deterministic access and self-starting behavior.

The first and primary effort is to engineer the deterministic access of the single DKS. This entails breaking the degeneracy or multistability of the single DKS and multiple DKS, i.e., guaranteeing single soliton generation as opposed to multiple soliton generation. This multistability breaking is necessary because the soliton number is effectively stochastic due to the modulation instability-seeded chaotic generation behavior [13]. Past approaches to isolate the single DKS have relied on delicate mode interactions or cascaded quadratic processes [14–18]. To make matters worse, typical thermal effects inhibit access to the single DKS through adiabatic pump modulation altogether. Because DKSs exist on the thermally unstable, red-detuned side of the cavity resonance, the relatively low-average power single soliton state is ordinarily thermally inaccessible when adiabatically detuning the pump laser across the resonance–the conventional means of accessing DKS states. At the cost of complexity, several methods have been developed to overcome this thermal issue including pump power modulation [19–21], abrupt power kicking [22, 23], and auxiliary laser assisted pumping [24]. However, these techniques do not break DKS multistability and address deterministic access. The second and more recent effort toward "turn-key" Kerr microcombs is to engineer self-starting behavior of solitons [25, 26]. These experiments seek to simplify the complicated, path dependent pump modulation schemes that generate solitons, so that successful DKS generation merely requires a CW pump laser at a static power and detuning. While these separate efforts represent significant steps towards scalable and robust Kerr microcombs, until now, deterministic access and self-starting behavior have not been satisfied simultaneously.

In this paper, we theoretically and numerically establish a means by which *both* deterministic access and self-starting of the single DKS are granted for the first time. We do this by exploiting the opposing interactions of a slow thermal response, and a fast, *negative*, Kerr nonlinearity. More specifically, under the conditions of thermal effects, normal dispersion, and a negative Kerr nonlinearity from the cascaded quadratic process [27], we graphically (Fig. 1) find a regime in which multistability is broken and deterministic single DKS access is guaranteed, and the underlying CW-only solution is unstable. Here, the single DKS is the only stable behavior. We term this novel operating regime

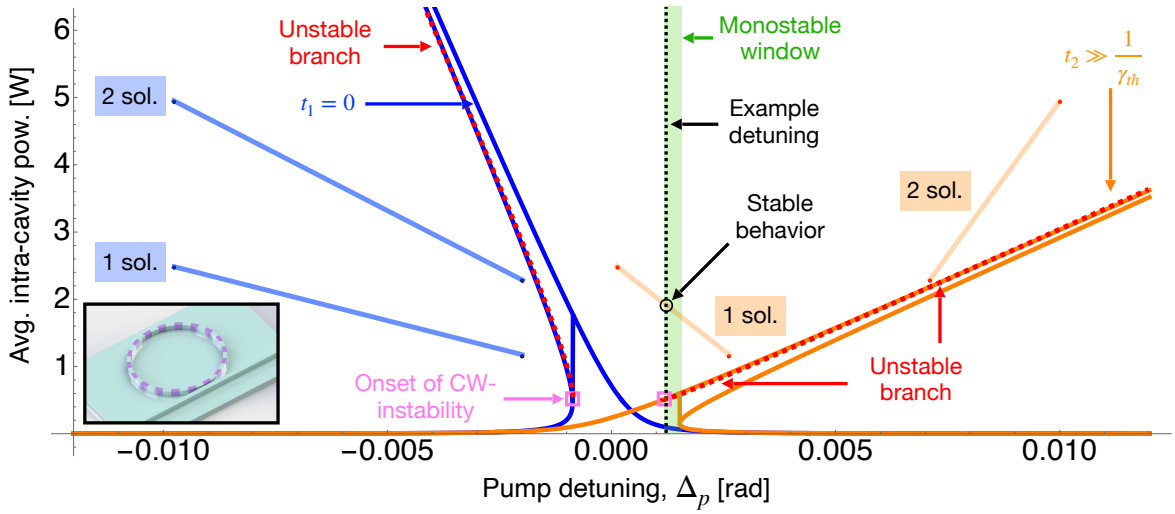

Fig. 1. Cavity resonance profile, illustrating the MS-DKS existence window shaded in green. The initial Kerr-only resonance profile and DKS states (lines marked 1 or 2 sol.) are plotted in blue, while the steady-state counterparts are plotted in orange. The unstable branches are marked by red dashed lines, and the instability onsets are marked by pink squares.

monostable-DKS (MS-DKS). We discuss design principles to access the MS-DKS state in periodically poled lithium niobate (PPLN) microresonators. We numerically demonstrate MS-DKS by solving the Lugiato-Lefever equation [28] alongside a cavity thermal dynamics equation [29]. We observe cycling through behaviors such as chaos, soliton states, and CW-only that settles into stable single soliton behavior, indicating self-starting and deterministic operation. Finally, we demonstrate the resilience of MS-DKS by rapidly perturbing the pump detuning and observing the reemergence of the single DKS.

2. MS-DKS CRITERIA

The three essential criteria that define MS-DKS are 1) to break the multistability of solitons, 2) to open up a monostable window, and 3) to position the single soliton existence range within the monostable window. Here, we define these criteria graphically, describing an example case.

In [13], Li *et al.* introduced a graphical method of determining soliton stability in order to predict whether the single soliton is adiabatically accessible in the presence of thermal effects. We build on this model in Fig. 1, plotting the analytically determined average power of the CW-only solution and DKS solutions as a function of pump detuning. To visualize the dynamics of cavity behavior, we plot the initial resonance profile affected only by the instantaneous Kerr nonlinearity (blue, t_1) and the steady-state resonance profile that also takes into account the delayed thermal response (orange, t_2). Details about the resonance profile construction, additional examples, and the cavity thermal dynamics are given in the Supplement Sections 1, 2, and 3.

To satisfy the first aforementioned criterion for MS-DKS, breaking multistability, the fast Kerr-induced resonance shift must *oppose* the slow thermally-induced resonance shift. Such a condition has not been satisfied in conventional Kerr combs until now. In our proposed PPLN platform (Supplement Sections 3 and 4), the necessary negative Kerr nonlinearity is achieved from the cascaded quadratic process [27]. DKS existence is guaranteed by normal dispersion waveguide design and the negative Kerr nonlinearity. We see in Fig. 1 that the opposing Kerr and thermal effects separate the single- and two-soliton existence ranges in the steady-state resonance profile (t_2), breaking multistability.

While opposing Kerr and thermal effects break the multistability between the single- and multi-soliton states, a stable CW-only solution can still co-exist at the same pump detuning. To satisfy the second criterion, opening up a monostable window, there must be a pump detuning range where stable CW-only solutions are forbidden. It is well known that the Kerr nonlinearity leads to an unstable branch of the cavity resonance profile (red dotted lines in Fig. 1), and thus the design goal here is to ensure that the unstable branch extends over a portion of the stable branch at steady state (green shaded area in Fig. 1 called the monostable window). This is made possible by the opposing fast Kerr and slow thermal effects, but the exact monostable window characteristics are determined by a variety of parameters as described later in Fig. 2.

To satisfy the third criterion, placing the single soliton existence range within the monostable window, the single DKS average power must be higher than the onset power of the CW instability (pink squares in Fig. 1). This arrangement allows the t_1 single soliton existence region to thermally shift into a t_2 position within the monostable window.

3. DESIGN PRINCIPLES

The most direct way to separate the single soliton from the double (and higher number) soliton existence regions is through a large thermal effect. However, discussed shortly, the strength of the thermal shift and the strength of the effective Kerr nonlinearity are co-constrained, and the thermal shift is not the most readily adjustable parameter because the effective Kerr nonlinearity must be generated though stringent cascaded $\chi^{(2)}$ processes (see Supplement Section 4). Instead, it is better to decrease the max detuning of the soliton state (Eq. S7), minimizing the soliton existence range, and thus lowering the thermal shift needed to separate the one and two soliton existence ranges. The simplest way to lower the maximum detuning is by lowering the pump power (as long as one is above threshold). Notably, this does not influence soliton characteristics. We also consider that there is an additional relationship between thermal shifts

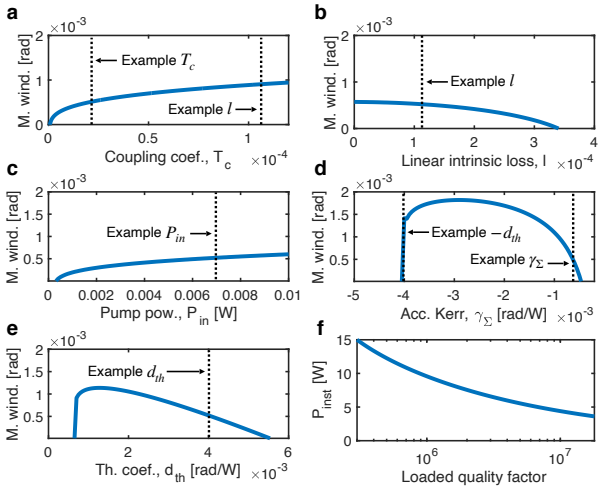

Fig. 2. Monostable window (M. wind.) analysis. (a) M. wind. vs. coupling coefficient, T_c. (b) M. wind. vs. intrinsic loss, l. (c) M. wind. vs. pump power, P_{in}. (d) M. wind. vs. accumulated Kerr nonlinearity, γ_Σ. Strength of the thermal shift coefficient, d_{th}, shown as well. (e) M. wind. vs. thermal shift coefficient, d_{th}. (f) P_{inst} vs. loaded quality factor when critically coupled.

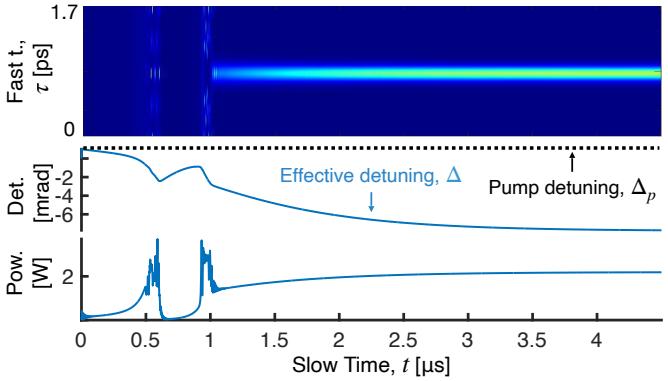

Fig. 3. (a) Top panel: heat map of MS-DKS formation. Middle panel: pump detuning (dotted line) and effective detuning (blue line). Lower panel: avg. intra-cavity power dynamics.

and the effective Kerr nonlinearity because changes in temperature affect the phase-matching conditions at the heart of the cascaded-quadratic nonlinearity; we discuss this in Supplement Section 5 and find that the effect is negligible.

We investigate the effects of various resonator parameters on the width of the monostable window (Fig. 2), varying one parameter individually from the example MS-DKS case (see Supplement Section 2). We find the monostable window by determining the minimum intra-cavity power at which CW-instability occurs, where the unstable central branch of the CW-solution meets the stable underlying branch. Once the location of this point is found, as shown by the pink squares in Fig. 1, the monostable window can be calculated as detailed in Supplement Section 7.

In Fig. 2a, we see that increasing the coupling coefficient, T_c, increases the monostable window. However, increasing sources of dissipation comes at a trade-off between increasing the monostable window and placing the single soliton inside the window discussed in the next subsection. l, the linear absorption loss, is shown for comparison. In Fig. 2b, as we increase l, the monostable window decreases until vanishing. In Fig. 2c, we find that the monostable window increases with pump power. However, as mentioned, increasing pump power comes with the trade-off of decreasing the separation between the single soliton and double soliton existence ranges. In Fig. 2d, we vary the accumulated Kerr nonlinearity $\gamma_\Sigma = \gamma L$, where γ is the effective nonlinear coefficient, and L is the resonator circumference. When $|\gamma_\Sigma|$ is greater than $|d_{th}|$, the effective thermal shift parameter, monostability cannot occur. While it may appear that increasing $|\gamma_\Sigma|$ closer to d_{th} would be beneficial in increasing the monostable window, much like increasing the pump power, increasing $|\gamma_\Sigma|$ counter-productively increases overlap between the single soliton and two soliton states. In practice, we find that MS-DKS operation is ideal when d_{th} is several times $|\gamma\Sigma|$. In Fig. 2e we vary the effective thermal shift parameter, d_{th}. At lower strengths, the monostable window briefly increases with d_{th}. After, the monostable window shrinks and eventually closes.

In order to position the single soliton in the monostable window, the average power of the single soliton must be greater than the power at which CW-instability begins. To achieve this inequality, one must increase DKS average power and/or decrease the CW-instability threshold. Increasing the DKS average power can be accomplished by increasing second order dispersion, which is governed by the device design. Lowering the Kerr inflection point can be accomplished by decreasing resonator losses–i.e. increasing loaded Q as shown in Fig. 2f.

Given resonator parameters (based on Z-cut LN) listed in Supplement Section 2, notably limited by a GVD of 400 fs^2/mm, we believe that quality factors of 30 million or higher are required to enter the regime of MS-DKS. Increasing the GVD of the cavity would, however, lower this requirement. We note that, presently, LN microresonators have not yet reached the material limit of LN which would push the quality factor well past 30 million (see Supplement Section 8).

4. NUMERICAL DEMONSTRATION AND DYNAMICS

We generate numerical simulations by solving the Lugiato-Lefever equation [28] simultaneously with a thermal rate equation through a split-step Fourier method (see Supplement Section 9). In Fig. 3, at $t = 0$ the pump is switched on and the pump detuning is held constant, as displayed in the central panel of Fig. 3. We observe that the pump shifts the cavity resonance and thus the effective detuning, which drives the cavity through a cycle of chaos and CW-only behavior (seen in upper and lower panels depicting heat map temporal evolution, and average-intracavity power evolution, respectively). Eventually, the cavity generates a single soliton, after which the cavity enters steady-state (longer and shorter-term views are in Supplement Section 10). A stable single soliton was always realized over hundreds of separate iterations beginning from randomized quantum noise.

We note that in the first chaotic cycle shown, a single soliton is not generated and the cavity reenters CW-only behavior, before resuming the chaotic behavior that precedes the single soliton. This cyclical behavior is a product of the instability of CW-only behavior which can be understood through Fig. 1. If a single soliton is not generated and the CW-only solution is accessed instead, the cavity undergoes repeating cycles in which the instantaneous profile shifts over to the long-term profile, reseeding soliton behavior until the single soliton is accessed.

Reliable Kerr comb operation requires resiliency against per-

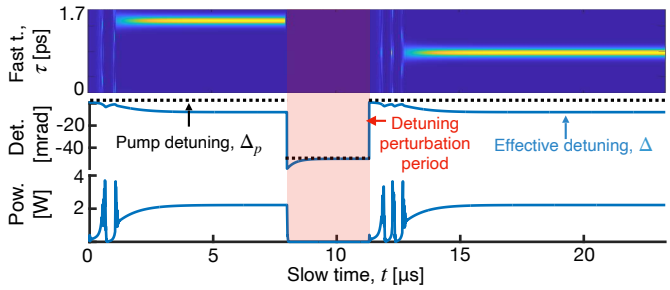

Fig. 4. Perturbation dynamics for MS-DKS.

turbation. In Fig. 4 we set the pump parameters to operate in the MS-DKS regime, observing the formation of the single soliton. After this formation, a sharp detuning step of 50 mrad lasting 3.3 ms destroys the soliton. But after the detuning has returned to within the MS-DKS regime, the single soliton is formed again (non-MS example in Supplement Section 10a for comparison).

5. CONCLUSION

In closing, we propose a new operating regime for DKS where multistability is broken, and the underlying CW solution is rendered unstable through the competing effects of a Kerr nonlinearity and counteracting, slow, power dependent resonance shift such as a thermal shift. Hence, in MS-DKS, the single soliton is self-starting and deterministic with a CW pump. We provide a graphical means of finding and analyzing this behavior through instantaneous and long-term resonance profiles. We give guidelines for how to access MS-DKS behavior beyond simply a negative Kerr nonlinearity and positive dispersion. This includes a high quality factor, relatively low pump powers, and a thermal effect several times stronger than the Kerr shift.

We emphasize that this regime *in general* is made possible through the interaction of a fast Kerr nonlinearity and a *much slower, counteracting*, average power-dependent shift. This is similar to recent experiments where the interaction of a Kerr effect and a slow photorefractive effect in lithium niobate grants bi-directional switching and deterministic access [25, 30]. One difference is that thermal effects are average power-dependent, whereas the photorefractive effect is intensity-dependent like the Kerr nonlinearity. Fundamentally, this difference leads to less coupling between the thermal shift and the Kerr shift, which widens the parameter space to access the MS-DKS regime.

The MS-DKS mechanism points to fundamentally enhanced reliability of Kerr microcombs [26]. This mechanism may also aid in the reliable generation of other interesting behaviors such as soliton breathers and soliton crystals. Our analysis suggests fruitful opportunities in exploring nonlinear optical behavior subject to counteracting shifts at very different timescales [25].

Funding. National Science Foundation (ECCS 2048202); Office of Naval Research (N00014-19-1-2251).

Acknowledgments. E. Tsao thanks K. Jia and S. Tsao, and acknowledges support from the National Defense Science and Engineering Graduate (NDSEG) Fellowship.

Disclosures. The authors declare no conflicts of interest.

Supplemental document. See Supplement 1 for supporting content.

REFERENCES

1. S. A. Diddams, K. Vahala, and T. Udem, Science **369**, 6501 (2020).
2. P. Del'Haye, A. Schliesser, O. Arcizet, T. Wilken, R. Holzwarth, and T. J. Kippenberg, Nature **450**, 1214 (2007).
3. P. Marin-Palomo, J. N. Kemal, M. Karpov, A. Kordts, J. Pfeifle, M. H. Pfeiffer, P. Trocha, S. Wolf, V. Brasch, M. H. Anderson, R. Rosenberger, K. Vijayan, W. Freude, T. J. Kippenberg, and C. Koos, Nature **546**, 274 (2017).
4. B. Corcoran, M. Tan, X. Xu, A. Boes, J. Wu, T. G. Nguyen, S. T. Chu, B. E. Little, R. Morandotti, A. Mitchell, and D. J. Moss, Nat. Commun. **11**, 1 (2020).
5. M. G. Suh, X. Yi, Y. H. Lai, S. Leifer, I. S. Grudinin, G. Vasisht, E. C. Martin, M. P. Fitzgerald, G. Doppmann, J. Wang, D. Mawet, S. B. Papp, S. A. Diddams, C. Beichman, and K. Vahala, Nat. Photonics **13**, 25 (2019).
6. E. Obrzud, M. Rainer, A. Harutyunyan, M. H. Anderson, J. Liu, M. Geiselmann, B. Chazelas, S. Kundermann, S. Lecomte, M. Cecconi, A. Ghedina, E. Molinari, F. Pepe, F. Wildi, F. Bouchy, T. J. Kippenberg, and T. Herr, Nat. Photonics **13**, 31 (2019).
7. P. Trocha, M. Karpov, D. Ganin, M. H. Pfeiffer, A. Kordts, S. Wolf, J. Krockenberger, P. Marin-Palomo, C. Weimann, S. Randel, W. Freude, T. J. Kippenberg, and C. Koos, Science **359**, 887 (2018).
8. M. G. Suh, Q. F. Yang, K. Y. Yang, X. Yi, and K. J. Vahala, Science **354**, 600 (2016).
9. S. W. Huang, J. Yang, M. Yu, B. H. McGuyer, D. L. Kwong, T. Zelevinsky, and C. W. Wong, Sci. Adv. **2**, e1501489 (2016).
10. E. Lucas, P. Brochard, R. Bouchand, S. Schilt, T. Südmeyer, and T. J. Kippenberg, Nat. Commun. **11**, 1 (2020).
11. K. Jia, X. Wang, D. Kwon, J. Wang, E. Tsao, H. Liu, X. Ni, J. Guo, M. Yang, X. Jiang, J. Kim, S.-n. Zhu, Z. Xie, and S.-W. Huang, Phys. Rev. Lett. **125**, 143902 (2020).
12. T. J. Kippenberg, A. L. Gaeta, M. Lipson, and M. L. Gorodetsky, Science **361**, 6402 (2018).
13. Q. Li, T. C. Briles, D. A. Westly, T. E. Drake, J. R. Stone, B. R. Ilic, S. A. Diddams, S. B. Papp, and K. Srinivasan, Optica **4**, 193 (2017).
14. A. W. Bruch, X. Liu, Z. Gong, J. B. Surya, M. Li, C. L. Zou, and H. X. Tang, Nat. Photonics **15**, 21 (2021).
15. X. Xue, X. Zheng, and B. Zhou, Photonics Res. **6**, 948 (2018).
16. C. Bao, Y. Xuan, D. E. Leaird, S. Wabnitz, M. Qi, and A. M. Weiner, Optica **4**, 1011 (2017).
17. H. Guo, M. Karpov, E. Lucas, A. Kordts, M. H. Pfeiffer, V. Brasch, G. Lihachev, V. E. Lobanov, M. L. Gorodetsky, and T. J. Kippenberg, Nat. Phys. **13**, 94 (2017).
18. M. Nie, Y. Xie, and S. W. Huang, Nanophotonics **10**, 1691 (2021).
19. S. B. Papp, P. Del'Haye, and S. A. Diddams, Opt. Express **21**, 17615 (2013).
20. P. Del'Haye, K. Beha, S. B. Papp, and S. A. Diddams, Phys. Rev. Lett. **112**, 1 (2014).
21. T. Wildi, V. Brasch, J. Liu, T. J. Kippenberg, and T. Herr, Opt. Lett. **44**, 4447 (2019).
22. V. Brasch, M. Geiselmann, M. H. P. Pfeiffer, and T. J. Kippenberg, Opt. Express **24**, 29312 (2016).
23. X. Yi, Q.-F. Yang, K. Youl Yang, and K. Vahala, Opt. Lett. **41**, 2037 (2016).
24. H. Zhou, Y. Geng, W. Cui, S.-W. Huang, Q. Zhou, K. Qiu, and C. Wei Wong, Light. Sci. & Appl. **8**, 50 (2019).
25. Y. He, Q.-F. Yang, J. Ling, R. Luo, H. Liang, M. Li, B. Shen, H. Wang, K. Vahala, and Q. Lin, Optica **6**, 1138 (2019).
26. B. Shen, L. Chang, J. Liu, H. Wang, Q.-F. Yang, C. Xiang, R. N. Wang, J. He, T. Liu, W. Xie, J. Guo, D. Kinghorn, L. Wu, Q.-X. Ji, T. J. Kippenberg, K. Vahala, and J. E. Bowers, Nature **582**, 365 (2020).
27. R. Desalvo, D. J. Hagan, G. Stegeman, and E. W. V. Stryland, Opt. Lett. **17**, 28 (1992).
28. S. Coen, H. G. Randle, T. Sylvestre, and M. Erkintalo, Opt. Lett. **38**, 37 (2013).
29. T. Carmon, L. Yang, and K. J. Vahala, Opt. Express **12**, 4742 (2004).
30. Z. Gong, X. Liu, Y. Xu, M. Xu, J. B. Surya, J. Lu, A. Bruch, C. Zou, and H. X. Tang, Opt. Lett. **44**, 3182 (2019).

FULL REFERENCES

1. S. A. Diddams, K. Vahala, and T. Udem, "Optical frequency combs: Coherently uniting the electromagnetic spectrum," Science **369**, 6501 (2020).
2. P. Del'Haye, A. Schliesser, O. Arcizet, T. Wilken, R. Holzwarth, and T. J. Kippenberg, "Optical frequency comb generation from a monolithic microresonator," Nature **450**, 1214–1217 (2007).
3. P. Marin-Palomo, J. N. Kemal, M. Karpov, A. Kordts, J. Pfeifle, M. H. Pfeiffer, P. Trocha, S. Wolf, V. Brasch, M. H. Anderson, R. Rosenberger, K. Vijayan, W. Freude, T. J. Kippenberg, and C. Koos, "Microresonator-based solitons for massively parallel coherent optical communications," Nature **546**, 274–279 (2017).
4. B. Corcoran, M. Tan, X. Xu, A. Boes, J. Wu, T. G. Nguyen, S. T. Chu, B. E. Little, R. Morandotti, A. Mitchell, and D. J. Moss, "Ultra-dense optical data transmission over standard fibre with a single chip source," Nat. Commun. **11**, 1–7 (2020).
5. M. G. Suh, X. Yi, Y. H. Lai, S. Leifer, I. S. Grudinin, G. Vasisht, E. C. Martin, M. P. Fitzgerald, G. Doppmann, J. Wang, D. Mawet, S. B. Papp, S. A. Diddams, C. Beichman, and K. Vahala, "Searching for exoplanets using a microresonator astrocomb," Nat. Photonics **13**, 25–30 (2019).
6. E. Obrzud, M. Rainer, A. Harutyunyan, M. H. Anderson, J. Liu, M. Geiselmann, B. Chazelas, S. Kundermann, S. Lecomte, M. Cecconi, A. Ghedina, E. Molinari, F. Pepe, F. Wildi, F. Bouchy, T. J. Kippenberg, and T. Herr, "A microphotonic astrocomb," Nat. Photonics **13**, 31–35 (2019).
7. P. Trocha, M. Karpov, D. Ganin, M. H. Pfeiffer, A. Kordts, S. Wolf, J. Krockenberger, P. Marin-Palomo, C. Weimann, S. Randel, W. Freude, T. J. Kippenberg, and C. Koos, "Ultrafast optical ranging using microresonator soliton frequency combs," Science **359**, 887–891 (2018).
8. M. G. Suh, Q. F. Yang, K. Y. Yang, X. Yi, and K. J. Vahala, "Microresonator soliton dual-comb spectroscopy," Science **354**, 600–603 (2016).
9. S. W. Huang, J. Yang, M. Yu, B. H. McGuyer, D. L. Kwong, T. Zelevinsky, and C. W. Wong, "A broadband chip-scale optical frequency synthesizer at 2.7 × 10-16 relative uncertainty," Sci. Adv. **2**, e1501489 (2016).
10. E. Lucas, P. Brochard, R. Bouchand, S. Schilt, T. Südmeyer, and T. J. Kippenberg, "Ultralow-noise photonic microwave synthesis using a soliton microcomb-based transfer oscillator," Nat. Commun. **11**, 1–8 (2020).
11. K. Jia, X. Wang, D. Kwon, J. Wang, E. Tsao, H. Liu, X. Ni, J. Guo, M. Yang, X. Jiang, J. Kim, S.-n. Zhu, Z. Xie, and S.-W. Huang, "Photonic Flywheel in a Monolithic Fiber Resonator," Phys. Rev. Lett. **125**, 143902 (2020).
12. T. J. Kippenberg, A. L. Gaeta, M. Lipson, and M. L. Gorodetsky, "Dissipative Kerr solitons in optical microresonators," Science **361**, 6402 (2018).
13. Q. Li, T. C. Briles, D. A. Westly, T. E. Drake, J. R. Stone, B. R. Ilic, S. A. Diddams, S. B. Papp, and K. Srinivasan, "Stably accessing octave-spanning microresonator frequency combs in the soliton regime," Optica **4**, 193 (2017).
14. A. W. Bruch, X. Liu, Z. Gong, J. B. Surya, M. Li, C. L. Zou, and H. X. Tang, "Pockels soliton microcomb," Nat. Photonics **15**, 21–27 (2021).
15. X. Xue, X. Zheng, and B. Zhou, "Soliton regulation in microcavities induced by fundamental–second-harmonic mode coupling," Photonics Res. **6**, 948 (2018).
16. C. Bao, Y. Xuan, D. E. Leaird, S. Wabnitz, M. Qi, and A. M. Weiner, "Spatial mode-interaction induced single soliton generation in microresonators," Optica **4**, 1011 (2017).
17. H. Guo, M. Karpov, E. Lucas, A. Kordts, M. H. Pfeiffer, V. Brasch, G. Lihachev, V. E. Lobanov, M. L. Gorodetsky, and T. J. Kippenberg, "Universal dynamics and deterministic switching of dissipative Kerr solitons in optical microresonators," Nat. Phys. **13**, 94–102 (2017).
18. M. Nie, Y. Xie, and S. W. Huang, "Deterministic generation of parametrically driven dissipative Kerr soliton," Nanophotonics **10**, 1691–1699 (2021).
19. S. B. Papp, P. Del'Haye, and S. A. Diddams, "Parametric seeding of a microresonator optical frequency comb," Opt. Express **21**, 17615 (2013).
20. P. Del'Haye, K. Beha, S. B. Papp, and S. A. Diddams, "Self-injection locking and phase-locked states in microresonator-based optical frequency combs," Phys. Rev. Lett. **112**, 1–6 (2014).
21. T. Wildi, V. Brasch, J. Liu, T. J. Kippenberg, and T. Herr, "Thermally stable access to microresonator solitons via slow pump modulation," Opt. Lett. **44**, 4447 (2019).
22. V. Brasch, M. Geiselmann, M. H. P. Pfeiffer, and T. J. Kippenberg, "Bringing short-lived dissipative Kerr soliton states in microresonators into a steady state," Opt. Express **24**, 29312 (2016).
23. X. Yi, Q.-F. Yang, K. Youl Yang, and K. Vahala, "Active capture and stabilization of temporal solitons in microresonators," Opt. Lett. **41**, 2037 (2016).
24. H. Zhou, Y. Geng, W. Cui, S.-W. Huang, Q. Zhou, K. Qiu, and C. Wei Wong, "Soliton bursts and deterministic dissipative Kerr soliton generation in auxiliary-assisted microcavities," Light. Sci. & Appl. **8**, 50 (2019).
25. Y. He, Q.-F. Yang, J. Ling, R. Luo, H. Liang, M. Li, B. Shen, H. Wang, K. Vahala, and Q. Lin, " Self-starting bi-chromatic LiNbO 3 soliton microcomb ," Optica **6**, 1138 (2019).
26. B. Shen, L. Chang, J. Liu, H. Wang, Q.-F. Yang, C. Xiang, R. N. Wang, J. He, T. Liu, W. Xie, J. Guo, D. Kinghorn, L. Wu, Q.-X. Ji, T. J. Kippenberg, K. Vahala, and J. E. Bowers, "Integrated turnkey soliton microcombs," Nature **582**, 365–369 (2020).
27. R. Desalvo, D. J. Hagan, G. Stegeman, and E. W. V. Stryland, "Self-focusing and self-defocusing by cascaded second-order effects in KTP," Opt. Lett. **17**, 28–30 (1992).
28. S. Coen, H. G. Randle, T. Sylvestre, and M. Erkintalo, "Modeling of octave-spanning Kerr frequency combs using a generalized mean-field Lugiato–Lefever model," Opt. Lett. **38**, 37 (2013).
29. T. Carmon, L. Yang, and K. J. Vahala, "Dynamical thermal behavior and thermal self- stability of microcavities," Opt. Express **12**, 4742–4750 (2004).
30. Z. Gong, X. Liu, Y. Xu, M. Xu, J. B. Surya, J. Lu, A. Bruch, C. Zou, and H. X. Tang, "Soliton microcomb generation at 2 μm in z-cut lithium niobate microring resonators," Opt. Lett. **44**, 3182 (2019).